IGBT-Module integrated Current and Temperature Sense Features based on Sigma-Delta Converter

Daniel Domes, Ulrich Schwarzer
Infineon Technologies AG, Max-Planck-Straße 5, 59581 Warstein, Germany

Abstract

System integration is one of the market driving issues in power electronics. In this paper the integration of precise shunts into IGBT modules, like it is done in Infineons MIPAQ^{TM} family, is compared to on-IGBT-chip current sense functionality. Temperature measurement via NTC-resistor on DBC-level or on-IGBT-chip integrated temp-sense-diodes will be treated as well. Further processing of the low voltage sense signals is done by sigma-delta converter including a functional isolation barrier by CorelessTransformerTechnology (CLT).

1. Introduction

Modern industrial inverter applications like precise high speed servo drives require accurately dosed electrical energy at high power levels provided by modern semiconductor inverter systems. For speed/torque control and protective functions of the drive system, several measurement points like instantaneous inverter output current, dc-link voltage, high power semiconductor junction temperature, etc. have to be captured during converter operation. Recent research, development effort and improvements in power electronics allow the integration of sense functionality into high power modules to reduce space, to increase the reliability and to save costs of the converter system. In this paper, two ways of integrating current and temperature measurement for control and protection functions will be shown, explained and discussed.

2. Integrating Current and Temperature Sense Solutions

The first approach is the integration of high power precise shunts into next generation IGBT modules. Temperature measurement is done by using common NTC-resistors. The second approach is the integration of temperature and current sense into the IGBT chip itself, realizing the Temperature-Current-Sense (TCS) IGBT.
The galvanic isolated transfer of the measurement signals to the digital control side is done by sigma-delta-conversion. The galvanic isolation barrier is formed by coreless-transformer-technology (CLT) [2, 3], which is integrated on-chip with the sigma-delta converter.

2.1. NTC & Shunt integrated IGBT Module

In Figure 1, the block diagram of the IGBT inverter full bridge module with integrated NTC, output current shunts and sigma-delta converters including galvanic isolation of digital signals is shown. This configuration is encapsulated by the proven Econo3 module case and belongs to the MIPAQ™ sense family [1].
Shunt measurement configurations for speed and torque control belongs to the least expensive solutions and can be easily soldered on the DBC inside the module. Doing this, the shunts can be easily isolated and cooled in an optimized way. The disadvantage of shunt measurement is the additional power dissipation, which is quite negligible as compared to the power semiconductor losses, however. A further drawback can be the reduced area on DBC level available for IGBT and diode dies.
Inside the module a NTC is integrated on the DBC. This configuration is proven and offers potential free temperature measurement. However, it does not provide a direct chip (IGBT/diode) related signal. For most drive applications it is sufficient to have a “low-pass-filtered” temperature information signal for observing IGBT temperature limits.
The voltage drop above the shunt is captured and digitalized via sigma-delta converter. Further features of small signal sigma-delta-conversion are treated below.

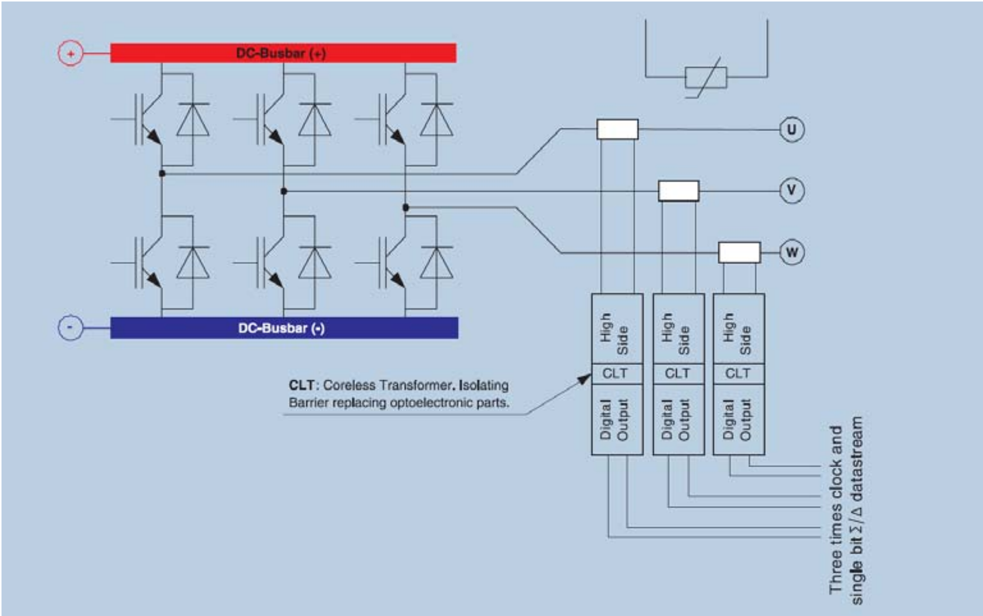

Fig. 1. Block diagram of the IGBT inverter full bridge module MIPAQ™ sense with integrated NTC, output current shunts and sigma-delta-converter including galvanic isolation for all digital signals

2.2. TCS-IGBT

The on-chip current sense functionality is achieved by separation of a defined number of IGBT cells from the power emitter metallization. Doing this, an additional sense emitter appears which should be connected to a low ohmic sense resistor (Figure 2).

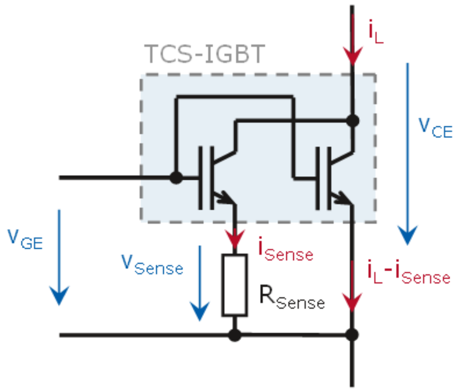

Fig. 2. Current-Sense-IGBT device (inside dashed line) with low ohmic sense resistor R_{Sense}

Thereby the sense current i_{Sense} is a fraction of the load current i_L of the whole device. Ideally i_{Sense} is only determined by the load current multiplied with the number of sense cells divided by the total cell number of the IGBT. So the measured sense current needs just to be multiplied by the cell number ratio in order to get the whole device current. The application of the sense resistor into the sense path causes a current density mismatch between the emitter-isolated sense cells and the main power cells. The higher the sense resistor value is, the higher the deviation between scaled sense voltage and measured load current becomes. On the other hand, for a appropriate voltage drop, a certain amount of sense resistance is required.

Figure 3 shows a 600V/200A sense IGBT ramping current in double pulse test. Choosing R_{Sense} to 0.5Ω, the nominal scaling is 50mV/div. Applying the nominal scaling for the v_{Sense} curve, the sense signal is something higher than the conventionally measured current curve i_L.

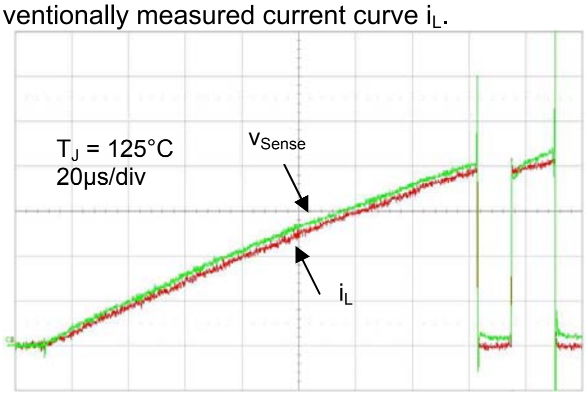

Fig. 3. 600V/200A TCS-IGBT: comparison of conventionally measured current i_L (red, 100A/div) and voltage drop v_{Sense} across a 0.5Ω sense resistor (green, 50mV/div)

Adjusting the deviation by a scaling factor of 0.9 for v_{Sense}, the situation like given in Fig. 4 appears. For smaller currents, the v_{Sense} curve fits the conventionally measured current curve. With increasing current, the sense voltage deviates more and more from the curve i_L. The reason behind this is, that the higher the voltage drop across the sense resistor becomes, the more the v_{CE} of the IGBTs sense cells and the power cells vary. This causes an increasing current density mismatch inside these cell parts leading to a lowered sense resistor voltage drop.

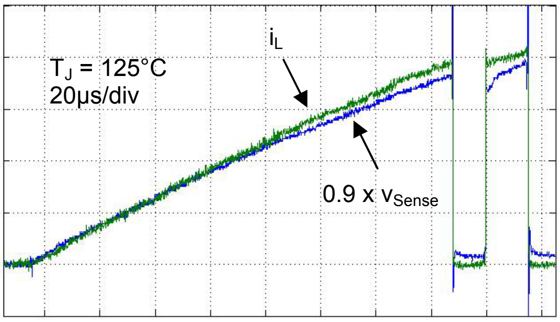

Fig. 4. data from Fig. 5, assuming a scaling factor of 0.9 for v_{Sense}

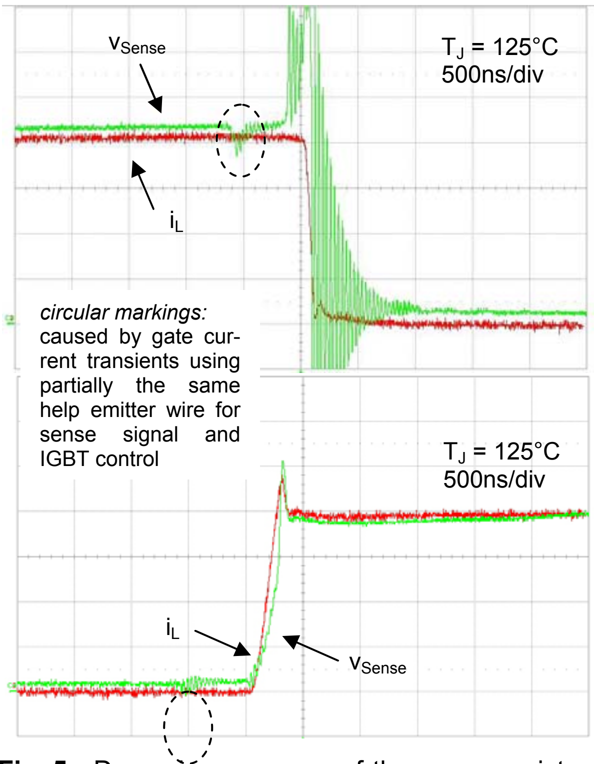

Fig. 5. Dynamic responses of the sense resistor voltage drop @ 2xIN: comparison of conventionally measured current iL (100A/div) and voltage drop vSense across a 0.5Ω sense resistor (50mV/div)

The dynamic responses of sense resistor voltage drop at switching 2 times the nominal current can be seen in Fig. 5. Turning-off the TCS-IGBT, the sense voltage reacts with ringing, but after 1µs the signal is stable. The turn-on process does not show any ringing. It reproduces the reverse recovery current peak of the diode in a qualitative manner followed by a transient 5µs undershoot (also visible in Fig. 3 and 4).

Summarizing, the current sense feature of the TCS-IGBT does not provide most precise current information like it is mandatory for electric machine control. But beside this, its performance in terms of accuracy and dynamic behaviour can be used for over-current and short-circuit-detection. Doing so, no additional high voltage diode is necessary like it is custom for conventional $v_{CE(sat)}$ detection. The sense signal is related to the emitter potential of each IGBT, allowing a simple approach of the current sense functionality. But one should keep in mind, that very small signals need to be handled for quite important protection functionality.

For temperature sense feature, on the top side of the TCS-IGBT there were pn-diodes integrated. In general, they are isolated from any potential appearing on the IGBT die, but their pn-junction voltage drop should be referred to emitter potential.

For constant current, the pn-junction voltage drop is a good indicator for the chip temperature. For investigating the diodes voltage step response to a thermal event in the chip, a 8µs short circuit was performed with the TCS-IGBT (Fig. 6).

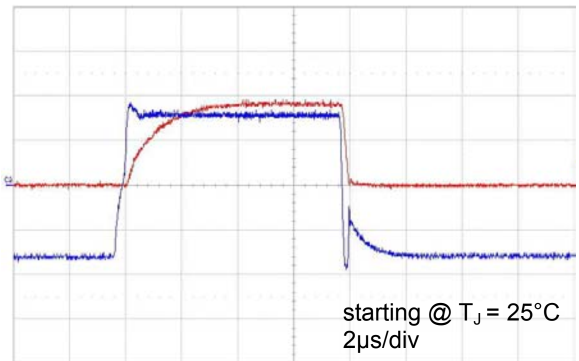

Fig. 6. Short circuit of the TCS-IGBT: gate emitter voltage (blue, 10V/div) and load current (red, 500A/div)

Figure 7 shows the changing in temp sense diode voltage drop as an answer of the short circuit event shown in Fig. 6. The internal heat peak reaches the diode after a delay of more than 100µs.

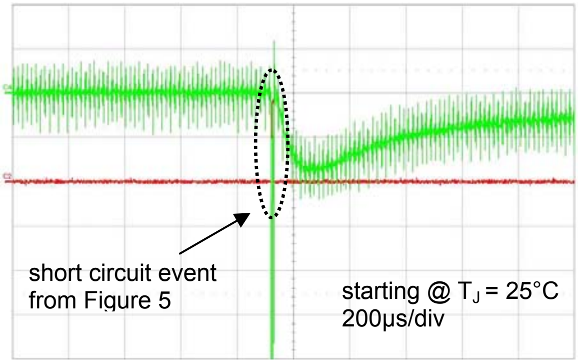

Fig. 7. Temp-Sense-Diode step response: changing in pn-junction voltage drop (green, 15mV/div) and load current (red, 500A/div)

Because of the thermal time constant inside the IGBT die, the temp sense feature seems not suitable to sense a short circuit. But apart from this, the temp sense feature provides a chip related and more or less integrated temperature information.

2.3. Sigma-Delta Converter with functional isolation capability

The sigma-delta conversion of the measurement signals generated by the above mentioned sense functions offer a big advantage compared to conventional A/D converter solutions. It only needs two channels for data streaming and clocking [4]. Both information lines easily can be galvanic isolated via micro transformer technology or so called CoreLessTransformer technology [2, 3]. Figure 8 shows the clock (f_{CLK} = 10 MHz) and the serial data waveforms of the Σ/Δ bit stream generated by the Infineon´s 2nd order sigma-delta converter IC type 1EC010I12-F. Latter includes a micro transformer isolation suitable for 1200V IGBT applications. The falling edge of the clock (Ch3, green) indicates the validity/"point of time" of the data stream.

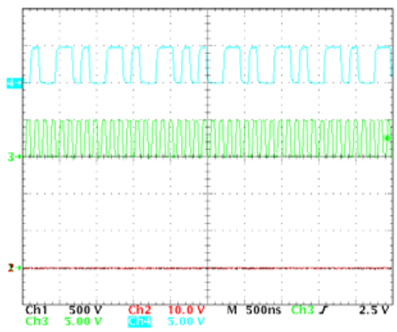

Fig. 8. Captured waveforms of the Σ/Δ converter 1EC010I12-F. Ch3: Clock (CLK) / Ch4: Serial Data Output (SD)

The so modulated and isolation-transmitted analogue measurement signal has to be digitally filtered before further processing in µC or in DSP for IGBT converter control. This sigma-delta modulated signal consists of its own origin frequency spectra plus quantization noise in the higher frequency region (see Figure 9b).

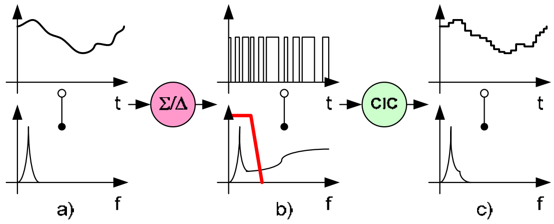

Fig. 9. Measurement signal depicted in time and frequency domain
a) before sigma-delta conversion
b) after sigma-delta conversion
c) after digital decimation filter process

Note, a narrow-band signal extraction from a wideband noised source has to be done. Therefore a digital filter with low-pass properties (red line in Figure 9b) has to be grind-in the transmission path between modulator output and converter control input. This filter also has to convert the modulated signal, toggling between "1" and "0" into parallel multi-bit words with length w and to divide down the high modulator clock speed (here: 10 MHz) for signal processing in µC/DSP. This normally require very fast multipliers, complex shift registers and long filter block chains which is often the largest bottleneck in a DSP system. Therefore here a very simple but efficient filter algorithm so called Cascaded-Integration-Comb (CIC) filter [5] is shown here, which can easily implemented into a FPGA. The CIC structure is depicted in Fig. 10.

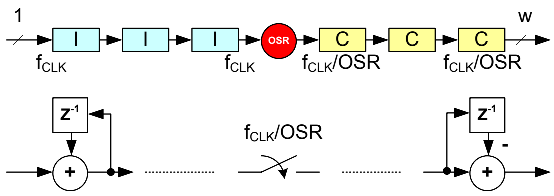

Fig. 10. Principle of a $k=3^{rd}$ order Cascaded-Integrator-Comb (CIC) filter

This filter structure consists of delay elements and adders which are working as integrators and differentiators and can be managed without multipliers. Between the integrators I and the combs C the clock f_{CLK} is divided by the decimation ratio OSR. At the output multi-bit word appears whose width w depends on the order k and OSR, which is described in [4]. OSR is equivalent to an oversampling of the captured sigma-delta input signal. Therefore only a simple 1st order RC low-pass filter has to be added to its input.

The time-discrete transfer function $H(z)$ in the z-domain can be described as follow:

$$H(z) = \frac{(1 - z^{-OSR})^k}{(1 - z^{-1})^k}$$

Here is k the order, OSR the oversampling/decimation ratio. The filter frequency transfer function $|H(f)|$ is a so called Sinc^k-function (sinus cardinalis):

$$|H(f)| = \left(\frac{1}{OSR} \cdot \frac{\sin(\pi f\, OSR/2)}{\sin(\pi f/2)}\right)^k$$

The sinc^3 filter response for an OSR = 16 is shown in Fig. 11.

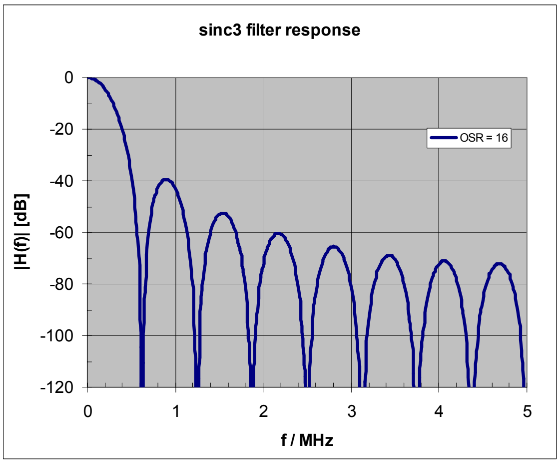

Fig. 11. sinc^3 filter response for an OSR = 16

Here, the -3dB point is located at f_{-3dB} = 164 kHz. This fulfills the required low-pass function depicted in Figure 9b). Further discussion about the Sinc^k-function transfer behavior is done in [5].

For testing and investigating the integrated Σ/Δ converter 1EC010I12-F transfer characteristics, a 1200V IGBT halfbridge output current was measured via a PEARSON-probe and the sigma-delta converter clock and bit stream signals were captured simultaneously. These waveforms are shown in Fig. 12. The captured waveforms were read from a personal computer spreadsheet calculation program, where the clock and bit stream signals were 1-bit-digitalized. With this spreadsheet program a 3rd order CIC filter structure, the Sinc^3 filter, was modeled to calculate line-by-line and simulative the status of the integrators and combs shown in Figure 10. This time-discrete filter processing represents an implementation into a FPGA. Here, different oversampling rates

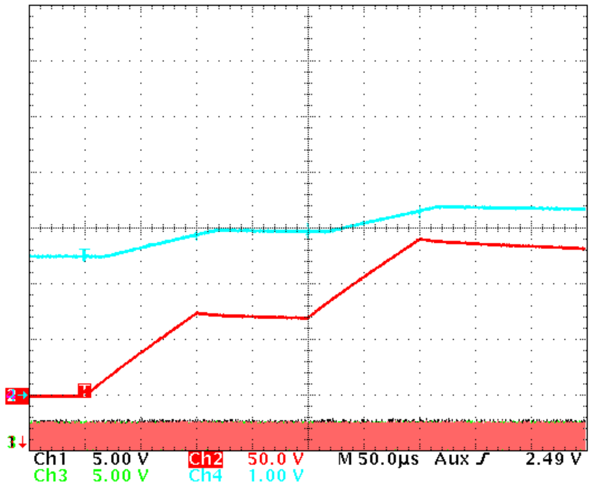

Fig. 12. Ch2: IGBT halfbridge output current (red, depicted in V instead of A) Ch1 + Ch3: sigma-delta converter output clock + bit stream ("noise" in the bottom) Ch4: internally filtered analogue output signal from 1EC010I12-F

(OSR) were chosen to clarify the different effects. In Fig. 13 the result after simulative digital filtering of the bit stream is shown. It clearly shows the nearly exact reconstruction of the sigma-delta modulated output current (the directly captured output current "I_pearson" waveform is covered by the filter output signals).

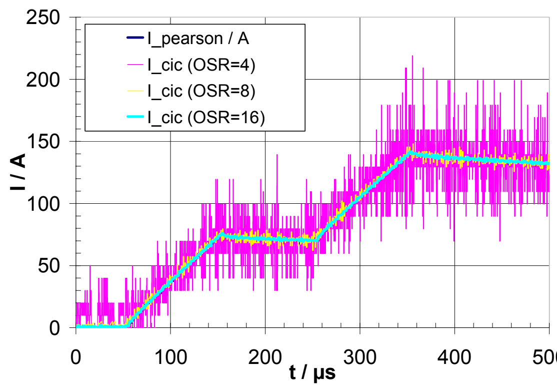

Fig. 13. Sinc^3-filtered sigma-delta modulation signal with different oversampling/decimation rates

The higher the oversampling/decimation rate OSR is, the more exact is the reconstructed signal and the longer the time response becomes. There is a linear trade-off between conversion speed t_{conv} and OSR with the assumption, the registers implemented in the FPGA are triggered by the sigma-delta clock of f_{CLK} = 10MHz (integrators I) or f_{CLK}/OSR (combs C) and the step response of the above mentioned sinc^3-filter was investigated:

$$t_{\mathrm{conv}} = \frac{4}{f_{\mathrm{CLK}}} \cdot \mathrm{OSR}$$

A trade-off between needed accuracy and conversion speed has to chosen for every application. Now the so decimated and filtered sigma-delta modulation signal can be used by the µC/DSP for power electronics application control. Further investigations and characterization of the integrated shunt/sigma-delta converter configuration are ongoing.

3. Conclusion

In this paper the future trend of integrating current and temperature measurement sense features inside IGBT modules, like it is realized with Infineon´s MIPAQ™ family, and even into IGBT chip devices is shown. In this study, two possible integration solutions were presented and explained. Their pros and cons were enumerated and discussed. In summary, shunt integration into IGBT modules is suitable for speed and torque control while the on-chip current sense seems to fit only for protection functions.

Compared with the NTC approach, the temp sense with on-chip-integrated diodes does not provide the proven low-passed temp signal but a chip related information. However, the NTC measurement signal is potential free, while the diode signal needs to be transferred by sigma-delta converter to the inverter control side.

Except for the NTC temp sense approach, the treated integration solutions small signals are digitalized and transmitted to the µC-/DSP-port via Σ/Δ converter including micro transformer technology for galvanic isolation. Compared to a classical converter with discrete sense equipment and digitalization units they are less expensive and more reliable.

4. Literature

[1] Schulz, M.; Kanschat, P.; Zhang, X.: „Higher Functionalities in Power Electronic Modules“, Bodo’s Power, September 2008, pp. 26 -28.

[2] Strzalkowski, B. et al.: “High performance IGBT-driver in microtransformer technology providing outstanding insulation capability”, Proceedings of PCIM 2003, Nürnberg, 2003.

[3] Strzalkowski, B.; Schwarzer, U.; Jansen, U.: “High performance IGBT-driver in microtransformer technology providing outstanding insulation capability”, Proceedings of PCIM2007, Nürnberg, 2003.

[4] Park, S.: “Principles of Sigma-Delta-Modulation for Analog-to-Digital Converters”, MOTOROLA Application Notes.

[5] Hogenauer, E. B.: “An Economial Class of Digital Filters for Decimation and Interpolation”, IEEE Transactions on Acoustics, Speech and Signal Processing, Volume 29, Issue 2, Apr 1981 pp. 155 - 162